Demand-Side Energy Storage System Management in Smart Grid

Wei-Yu Chiu, *Member, IEEE*, Hongjian Sun, *Member, IEEE*, and H. Vincent Poor, *Fellow, IEEE*

***Abstract*—An economical way to manage demand-side energy storage systems in the smart grid is proposed by using an H_∞ design. The proposed design can adjust the stored energy state economically according to the price signal, while tolerating a certain degree of system uncertainty and having physical constraints on the stored energy level satisfied. Roughly speaking, batteries in the proposed design are charged during a low-price period while being discharged during a high-price period for cost control. Simulations show that the proposed energy storage system can meet the real-time power demand and save money in the long term in contrast to energy storage systems using constant-state schemes.**

I. Introduction

The smart grid concept has attracted much attention recently due to increasing electricity demand and installation of renewable energy sources (RESs) such as solar panels and wind turbines. To have a manageable scale of system behavior, demand-side management (DSM) is becoming one of the most important research topics in the smart grid community. Via DSM, load shifting [1] has been considered as a means of adjusting power demand to reduce the peak load [2] or the peak-to-average ratio [3], [4]. Loads that are suitable for load shifting management include water heaters, washing machines or dishwashers, plug-in electric vehicles, refrigerators, air conditioners (thermostatic loads [5]), etc.

However, a significant fraction of power demand is not suitable for load shifting DSM, e.g., cooking, lighting, entertainment appliances [6], etc. In this case, it is still desirable to meet the demand economically based on the real-time price. This situation is considered in this work, and an economical way to manage it is proposed and carried out by the underlying distributed energy storage system in the smart grid. In practice, the stored energy state of each user is controlled to respond to the time-varying price signal.

In previous work, although several energy storage management schemes were proposed to achieve a prescribed working level [7] or a time-varying energy level [8], the price signal was not incorporated into the choice of such a desired level. In this work, the energy state of the storage system is constrained by the storage capacity as an upper bound and the required energy level for emergencies as a lower bound. The energy storage system is also managed in the presence of system uncertainty, i.e., not knowing the exact energy storage efficiency and the exact loss rate for power transmission among users. Therefore, this study is different from the cases studied in [7] and [8] due to its consideration of economical management, physical constraints on the storage state, and system uncertainty.

Most recently, noncooperative game theory approaches were proposed to address DSM problems in the smart grid [9]. In [3], Nguyen *et al.* considered an approach that minimizes the peak-to-average ratio in a distributed energy storage system, and a pricing model was investigated. In contrast to a noncooperative design, a cooperative DSM system was proposed in [10] to improve the energy utilization efficiency. Cooperative smart grid networks were also considered in [11] to reduce average power losses over distribution power lines. In this study, we propose a flexible demand-side energy storage system, which is suitable for either cooperative or noncooperative design. We will show that these two cases can be dealt with in our proposed framework by simply using different topology matrices.

The main contributions of this study are as follows. This work introduces H_∞ control techniques to the smart grid community. In the proposed energy storage system design, a flexible scheme is available for cooperative or noncooperative cases. Unlike existing work on energy storage system management using control theory, the proposed system incorporates the price signal into the adjustment of the stored energy level, and it is robustly designed against system uncertainty based on the H_∞ performance criterion.

The following notation is used throughout this study. $\boldsymbol{P} \succ 0$ means that $\boldsymbol{P}$ is a symmetric and positive-definite matrix. $[\boldsymbol{A}]_{ij}$ denotes the (i,j)-entry of the matrix $\boldsymbol{A}$. Similarly, for a column vector $\boldsymbol{x}$, $[\boldsymbol{x}]_i$ represents the ith element of the vector $\boldsymbol{x}$. For $\boldsymbol{P} \succ 0$, we define the induced norm $||\boldsymbol{x}||_{\boldsymbol{P}} := \sqrt{\boldsymbol{x}^T \boldsymbol{P} \boldsymbol{x}}$. The notation $||\cdot||$ denotes the Euclidean norm, i.e., $||\boldsymbol{x}||^2 = \boldsymbol{x}^T \boldsymbol{x}$.

The rest of the paper is organized as follows. Section II describes the dynamics of energy storage systems in the smart grid. The proposed control law for energy storage management is presented in Section III. Our simulation results are carried out in Section IV to confirm the validity of the proposed approach. Finally, we conclude this study in Section V.

II. System Model

This section presents a smart grid network that consists of a power grid and power consumers or users. The power grid is a conventional power provider to users, and a user could

W.-Y. Chiu and H. V. Poor are with the Department of Electrical Engineering, Princeton University, Princeton, NJ, 08544 USA (e-mail: wchiu@princeton.edu; poor@princeton.edu).

H. Sun is with the Division of Engineering, Kings College London, WC2R 2LS London, U.K. (e-mail: hongjian.sun@kcl.ac.uk).

This work was supported in part by the National Science Council of Taiwan under grant NSC100-2917-I-564-014, and in part by the U.S. Air Force Office of Scientific Research under MURI Grant FA9550-09-1-0643.

978-1-4673-0911-0/12/$31.00 ©2012 IEEE

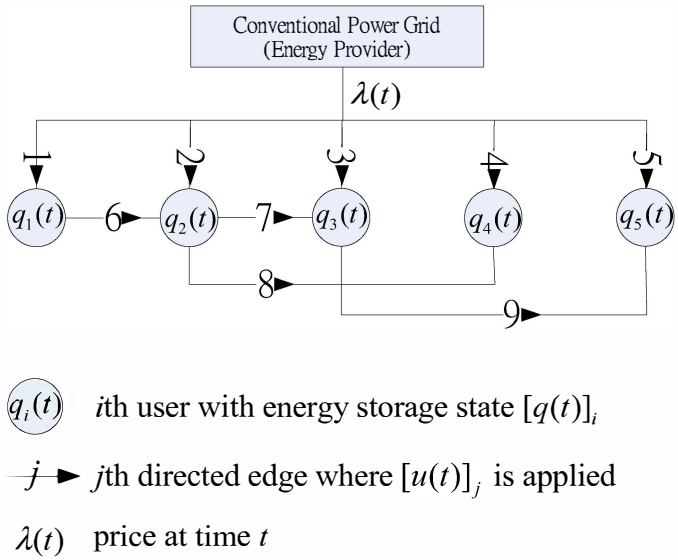

Fig. 1. An example of smart grid topology with $N = 5$ users and $L = 9$ edges.

be a smart house that intends to use energy efficiently. Each user is connected to the power grid and it may also have the connection with another user so that power can be controlled to flow among users.

See Fig. 1 as an example of a smart grid network. There are $N = 5$ users connected by $L = 9$ edges. Let $\boldsymbol{q}(t) \in \mathbb{R}^N$ and $\boldsymbol{u}(t) \in \mathbb{R}^L$ denote the energy stored in users' energy storage system and the power flow on the edges at time t, respectively. In our scheme, $[\boldsymbol{u}(t)]_j > 0$ implies that the power flow follows the direction indicated by the arrowed edge. For example, $[\boldsymbol{u}(t)]_6 > 0$ in Fig. 1 means user 1 is transmitting power to user 2 at time t. Conversely, if $[\boldsymbol{u}(t)]_6 < 0$, then user 2 is transmitting power to user 1 at time t. For the edges connecting users and the energy provider, $[\boldsymbol{u}(t)]_i > 0$ is interpreted as the case in which user i is buying power from the power grid, while $[\boldsymbol{u}(t)]_i < 0$ represents that user i is selling power to the power grid. For convenience, we always label the edges connecting users to the power grid by smaller numbers, i.e., $[\boldsymbol{u}(t)]_j$ for $j = 1, 2, ..., N$ control the power bought from or sold to the power grid. See Fig. 1 as an example. For the power price $\lambda(t)$, the total money spent or earned by a particular network at time t is $\lambda(t) \sum_{j=1}^{N} [\boldsymbol{u}(t)]_j$.

To describe the network topology, a topology matrix $\boldsymbol{B}(\beta)$ is used to indicate the users' connections, where $[\boldsymbol{B}(\beta)]_{ij}$ represents the connection of the jth edge to the ith user. We define $\boldsymbol{B}(\beta)$ as

$$[\boldsymbol{B}(\beta)]_{ij} = \begin{cases} 1, & \text{if edge } j \text{ connects user } i \text{ and the energy provider} \\ \beta, & \text{if edge } j \text{ connects two users and ends at user } i \\ -1, & \text{if edge } j \text{ connects two users and departs at user } i \\ 0, & \text{otherwise} \end{cases} \quad (1)$$

where $i = 1, 2, ..., N$ and $j = 1, 2, ..., L$. In (1), the power loss when transmitting power between users is modeled by the parameter β, where $1 > \beta > 0$. In other words, if one unit of power is transmitted from user i to user j, then user j receives only a fraction β of that unit of power. In this study, the exact value of β is unknown, but the range $[\beta_m, \beta_M]$ to which β belongs is available. For the network in Fig. 1, the topology matrix, according to (1), can be described as

$$\boldsymbol{B}(\beta) = \begin{bmatrix} 1 & 0 & 0 & 0 & 0 & -1 & 0 & 0 & 0 \\ 0 & 1 & 0 & 0 & 0 & \beta & -1 & -1 & 0 \\ 0 & 0 & 1 & 0 & 0 & 0 & \beta & 0 & -1 \\ 0 & 0 & 0 & 1 & 0 & 0 & 0 & \beta & 0 \\ 0 & 0 & 0 & 0 & 1 & 0 & 0 & 0 & \beta \end{bmatrix}. \quad (2)$$

Remark 1: We have assumed that each user is connected to the power grid. For a cooperative network, users may be connected to one another and each user is assumed to have sufficient capacity so that the power transmission among connected users becomes possible. Therefore, we have $L > N$ and the knowledge of energy states is used to control the power flow among users. By contrast, for a noncooperative case, we have $L = N$ and consider the situation in which the power transmission among users is impractical due to physical constraints in certain real-world scenarios. In this case, users are linked only to the power grid and there is no connection among users, i.e., users are allowed to exchange power only with the power grid. The proposed scheme is flexible in the sense that the proposed energy storage system is designed to fit both cooperative and noncooperative cases. The only difference results from using different topology matrices $\boldsymbol{B}(\beta)$ defined in (1)

For a particular topology $\boldsymbol{B}(\beta)$, the energy stored or consumed at users due to power control $\boldsymbol{u}(t)$ is $\boldsymbol{B}(\beta)\boldsymbol{u}(t)$. Let us denote by $\boldsymbol{x}(t) \in \mathbb{R}^N$ the power demand at time t and suppose that each user is equipped with RESs, e.g., solar panels, and hence extra power $\boldsymbol{v}(t) \in \mathbb{R}^N$ is available to users. The dynamics of this energy storage system can then be described as

$$\boldsymbol{q}(t+1) = \boldsymbol{A}(\alpha)\boldsymbol{q}(t) + [\boldsymbol{B}(\beta)\boldsymbol{u}(t) - \boldsymbol{x}(t) + \boldsymbol{v}(t)]\Delta t \quad (3)$$

with $\Delta t = 1$, $\boldsymbol{q}(t) \geq 0, \boldsymbol{x}(t) \geq 0$ and $\boldsymbol{v}(t) \geq 0$. In (3), $\boldsymbol{A}(\alpha)$ is termed a storage efficiency matrix and its value depends on the types of storage media that are used. In this study, $\boldsymbol{A}(\alpha) = \alpha \boldsymbol{I}_N$ is assumed with an unknown parameter $\alpha \approx 1$, where the uncertainty can be expressed as $\alpha \in [\alpha_m, \alpha_M]$ with given values of α_m and α_M.

As any storage system has a finite storage capacity, we use $\boldsymbol{q}_M$ to represent the maximum energy that can be stored by users. To deal with emergency situations, a minimum energy state $\boldsymbol{q}_m$ should be maintained at any time. Therefore, we have

$$\infty > \boldsymbol{q}_M \geq \boldsymbol{q}(t) \geq \boldsymbol{q}_m > 0 \quad (4)$$

for any time t due to physical and operational constraints. In the next section, demand-side energy storage management is considered, which is concerned with controlling the storage

system such that the power demand and physical storage constraints are satisfied in an economical way.

III. Proposed Energy Storage Management System

To facilitate energy storage management, this section introduces a dynamical system of desired energy states $\boldsymbol{q_r}(t) \in \mathbb{R}^N$. The power flow $\boldsymbol{u}(t)$ is designed so that $\boldsymbol{q_r}(t) \in [\boldsymbol{q}_m, \boldsymbol{q}_M]$ and $\boldsymbol{q}(t) \to \boldsymbol{q_r}(t)$. Two price thresholds λ_m and λ_M are used so that $\boldsymbol{q_r}(t) \to \boldsymbol{q}_M$ if $\lambda(t) \le \lambda_m$ while $\boldsymbol{q_r}(t) \to \boldsymbol{q}_m$ if $\lambda(t) \ge \lambda_M$. Roughly speaking, the basic idea is that the batteries in the energy storage system are charged/discharged when the price is below/above a predefined threshold. By doing so, energy is bought at a low price while being provided to the users when the price is high, i.e., economical demand-side management is achieved.

The desired energy state $\boldsymbol{q_r}(t)$ is designed as

$$\boldsymbol{q_r}(t+1) = \boldsymbol{A_r}\boldsymbol{q_r}(t) + \boldsymbol{r}(t) \tag{5}$$

where $\boldsymbol{A_r} \in \mathbb{R}^{N\times N}$ is a diagonal matrix with $0 < [\boldsymbol{A_r}]_{ii} < 1$, and $\boldsymbol{r}(t) \in \mathbb{R}^N$ is termed a reference input. The physical meaning of (5) is explained as follows. Let us suppose that the energy state $\boldsymbol{a}$ is desired to be reached. The reference input can then be chosen as $\boldsymbol{r}(t) = (\boldsymbol{I}_N - \boldsymbol{A_r})\boldsymbol{a}$ and the resulting error dynamics can be obtained as

$$\begin{aligned} &\boldsymbol{q_r}(t+1) - \boldsymbol{a} \\ &= \boldsymbol{A_r}\boldsymbol{q_r}(t) + (\boldsymbol{I}_N - \boldsymbol{A_r})\boldsymbol{a} - \boldsymbol{a} \\ &= \boldsymbol{A_r}(\boldsymbol{q_r}(t) - \boldsymbol{a}) \to \boldsymbol{0} \text{ as } t \to \infty. \end{aligned} \tag{6}$$

Therefore, controlling the reference input $\boldsymbol{r}(t)$ can lead to any desired states.

Referring to (4), we design $\boldsymbol{r}(t)$ in (5) as

$$\boldsymbol{r}(t) = \begin{cases} (\boldsymbol{I}_N - \boldsymbol{A_r})\boldsymbol{q}_m, & \text{if } \lambda(t) \ge \lambda_M \\ (\boldsymbol{I}_N - \boldsymbol{A_r})\boldsymbol{q}_M, & \text{if } \lambda(t) \le \lambda_m \\ (\boldsymbol{I}_N - \boldsymbol{A_r})\boldsymbol{q_r}(t), & \text{otherwise} \end{cases} \tag{7}$$

where λ_M and λ_m are two prescribed price thresholds, which generally depend on the distribution of $\lambda(t)$. The remaining work is to design $\boldsymbol{u}(t)$ in (3) so that $\boldsymbol{q}(t) \to \boldsymbol{q_r}(t)$ and hence, $\boldsymbol{q}(t)$ can reach desired states.

To facilitate the design of $\boldsymbol{u}(t)$, (5) is substituted into (3) and the tracking error dynamics $\boldsymbol{e}(t)$ can be obtained as

$$\begin{aligned} \boldsymbol{e}(t+1) &= \boldsymbol{q}(t+1) - \boldsymbol{q_r}(t+1) \\ &= \boldsymbol{A}(\alpha)(\boldsymbol{q}(t) - \boldsymbol{q_r}(t)) + \boldsymbol{B}(\beta)\boldsymbol{u}(t) \\ &\quad + (\boldsymbol{A}(\alpha) - \boldsymbol{A_r})\boldsymbol{q_r}(t) - \boldsymbol{r}(t) - \boldsymbol{x}(t) + \boldsymbol{v}(t) \\ &= \boldsymbol{A}(\alpha)\boldsymbol{e}(t) + \boldsymbol{B}(\beta)\boldsymbol{u}(t) + \boldsymbol{w}(\alpha, t) \end{aligned} \tag{8}$$

where

$$\boldsymbol{w}(\alpha, t) = (\boldsymbol{A}(\alpha) - \boldsymbol{A_r})\boldsymbol{q_r}(t) - \boldsymbol{r}(t) - \boldsymbol{x}(t) + \boldsymbol{v}(t).$$

Define $\bar{\beta} = (\beta_M + \beta_m)/2$ and $\bar{\alpha} = (\alpha_M + \alpha_m)/2$. Based on (8), we propose the control law

$$\boldsymbol{u}(t) = -\boldsymbol{B}^\dagger(\bar{\beta})\boldsymbol{w}(\bar{\alpha}, t) + \boldsymbol{K}\boldsymbol{e}(t) \tag{9}$$

where $\boldsymbol{B}(\bar{\beta})^\dagger$ represents the pseudo-inverse of $\boldsymbol{B}(\bar{\beta})$ and $\boldsymbol{K} \in R^{N\times N}$ is termed a control gain to be designed. The idea we introduce here is to use the term $-\boldsymbol{B}^\dagger(\bar{\beta})\boldsymbol{w}(\bar{\alpha}, t)$ in (9) to cancel the term $\boldsymbol{w}(\alpha, t)$ in (8), while the remaining term $\boldsymbol{K}\boldsymbol{e}(t)$ in (9) is combined with $\boldsymbol{A}(\alpha)\boldsymbol{e}(t)$ in (8) to ensure the convergence of $\boldsymbol{e}(t)$.

By substituting (9) into (8), the tracking error dynamics can be further expressed as

$$\boldsymbol{e}(t+1) = (\boldsymbol{A}(\alpha) + \boldsymbol{B}(\beta)\boldsymbol{K})\boldsymbol{e}(t) + \Delta\boldsymbol{w}(t) \tag{10}$$

where

$$\Delta\boldsymbol{w}(t) = \boldsymbol{w}(\alpha, t) - \boldsymbol{B}(\beta)\boldsymbol{B}(\bar{\beta})^\dagger\boldsymbol{w}(\bar{\alpha}, t).$$

Our energy storage management problem becomes equivalent to finding $\boldsymbol{K}$ such that $\boldsymbol{e}(t)$ converges to the all-zero state. In this case, we consider a control problem in which the system state $\boldsymbol{e}(t)$ is desired to be driven to zero in the presence of system disturbances $\Delta\boldsymbol{w}(t)$.

As the parameters α and β are unknown, a design that is robust against disturbances is needed. To this end, we consider the H_∞ performance criterion [12], [13]

$$V(t+1) - V(t) + \boldsymbol{e}(t)^T\boldsymbol{e}(t) - \rho^2\Delta\boldsymbol{w}(t)^T\Delta\boldsymbol{w}(t) < 0 \tag{11}$$

where $V(t) \ge 0$ and $\rho > 0$ are a Lyapunov function and an H_∞ attenuation level, respectively. A smaller value of ρ results in better tracking performance.

Remark 2: For a better understanding of (11), suppose the initial state is zero, i.e., $\boldsymbol{e}(0) = \boldsymbol{0}$ and thus $V(0) = 0$. According to (11) and noting that $V(t) \ge 0$ for any t, we have

$$\sum_{t=0}^{t_f} \boldsymbol{e}(t)^T\boldsymbol{e}(t) < \rho^2 \sum_{t=0}^{t_f} \Delta\boldsymbol{w}(t)^T\Delta\boldsymbol{w}(t) \tag{12}$$

for any positive t_f. The attenuation level ρ is thus desired to be as small as possible so that the tracking error energy $\sum_{t=0}^{t_f} \boldsymbol{e}(t)^T\boldsymbol{e}(t)$ can be attenuated at least down to $\rho^2 \sum_{t=0}^{t_f} \Delta\boldsymbol{w}(t)^T\Delta\boldsymbol{w}(t)$. This suggests that $\boldsymbol{K}$ should be designed in consideration of (11) while minimizing ρ^2.

Let us consider a quadratic Lyapunov function $V(t) = \boldsymbol{e}(t)^T\boldsymbol{P}\boldsymbol{e}(t)$ with some $\boldsymbol{P} \succ 0$ and $\boldsymbol{e}(t)$ expressed in (10). The left-hand side of (11) is then equal to

$$\begin{aligned} &||\boldsymbol{e}(t+1)||^2_{\boldsymbol{P}} - ||\boldsymbol{e}(t)||^2_{\boldsymbol{P}} + ||\boldsymbol{e}(t)||^2 - \rho^2||\Delta\boldsymbol{w}(t)||^2 \\ &= ||(\boldsymbol{A}(\alpha) + \boldsymbol{B}(\beta)\boldsymbol{K})\boldsymbol{e}(t) + \Delta\boldsymbol{w}(t)||^2_{\boldsymbol{P}} - ||\boldsymbol{e}(t)||^2_{\boldsymbol{P}} + ||\boldsymbol{e}(t)||^2 \\ &\quad - \rho^2||\Delta\boldsymbol{w}(t)||^2 \\ &= \begin{bmatrix} \boldsymbol{e}(t) \\ \Delta\boldsymbol{w}(t) \end{bmatrix}^T \left\{ \begin{bmatrix} (\boldsymbol{A}(\alpha) + \boldsymbol{B}(\beta)\boldsymbol{K})^T & \boldsymbol{I}_N \\ \boldsymbol{I}_N & \boldsymbol{0} \end{bmatrix} \begin{bmatrix} \boldsymbol{P} & \star \\ \boldsymbol{0} & \boldsymbol{I}_N \end{bmatrix} \right. \\ &\quad \times \begin{bmatrix} (\boldsymbol{A}(\alpha) + \boldsymbol{B}(\beta)\boldsymbol{K})^T & \boldsymbol{I}_N \\ \boldsymbol{I}_N & \boldsymbol{0} \end{bmatrix}^T - \left. \begin{bmatrix} \boldsymbol{P} & \star \\ \boldsymbol{0} & \rho^2\boldsymbol{I}_N \end{bmatrix} \right\} \\ &\quad \times \begin{bmatrix} \boldsymbol{e}(t) \\ \Delta\boldsymbol{w}(t) \end{bmatrix} \\ &:= \begin{bmatrix} \boldsymbol{e}(t) \\ \Delta\boldsymbol{w}(t) \end{bmatrix}^T \boldsymbol{\Phi}(\alpha, \beta) \begin{bmatrix} \boldsymbol{e}(t) \\ \Delta\boldsymbol{w}(t) \end{bmatrix}. \end{aligned} \tag{13}$$

In (13), "$\star$" denotes the term induced by symmetry, which notation will be used throughout this study.

It can be noted that if

$$\boldsymbol{\Phi}(\alpha, \beta) \prec 0 \tag{14}$$

then the H_∞ performance criterion (11) is satisfied. Using Schur complements [12], the condition (14) is equivalent to

$$\begin{bmatrix} \boldsymbol{P} & \star & \star & \star \\ \boldsymbol{0} & \rho^2 \boldsymbol{I}_N & \star & \star \\ \boldsymbol{A}(\alpha)+\boldsymbol{B}(\beta)\boldsymbol{K} & \boldsymbol{I}_N & \boldsymbol{P}^{-1} & \star \\ \boldsymbol{I}_N & \boldsymbol{0} & \boldsymbol{0} & \boldsymbol{I}_N \end{bmatrix} \succ 0. \tag{15}$$

Applying the congruent transformation [14] with $diag\{[\boldsymbol{P}^{-1}, \boldsymbol{I}_N, \boldsymbol{I}_N, \boldsymbol{I}_N]\}$ to (15), we have

$$\begin{bmatrix} \boldsymbol{P}^{-1} & \star & \star & \star \\ \boldsymbol{0} & \rho^2 \boldsymbol{I}_N & \star & \star \\ \boldsymbol{A}(\alpha)\boldsymbol{P}^{-1}+\boldsymbol{B}(\beta)\boldsymbol{K}\boldsymbol{P}^{-1} & \boldsymbol{I}_N & \boldsymbol{P}^{-1} & \star \\ \boldsymbol{P}^{-1} & \boldsymbol{0} & \boldsymbol{0} & \boldsymbol{I}_N \end{bmatrix} \succ 0. \tag{16}$$

By using change of variables with $\boldsymbol{Q} = \boldsymbol{P}^{-1}$ and $\boldsymbol{Y} = \boldsymbol{K}\boldsymbol{P}^{-1}$, the condition (16) can be transformed into

$$\boldsymbol{\Theta}(\alpha,\beta) := \begin{bmatrix} \boldsymbol{Q} & \star & \star & \star \\ \boldsymbol{0} & \rho^2 \boldsymbol{I}_N & \star & \star \\ \boldsymbol{A}(\alpha)\boldsymbol{Q}+\boldsymbol{B}(\beta)\boldsymbol{Y} & \boldsymbol{I}_N & \boldsymbol{Q} & \star \\ \boldsymbol{Q} & \boldsymbol{0} & \boldsymbol{0} & \boldsymbol{I}_N \end{bmatrix} \succ 0. \tag{17}$$

However, the parameters α and β are unknown and hence, (17) is not directly solvable. Since $\alpha \in [\alpha_m, \alpha_M]$ and $\beta \in [\beta_m, \beta_M]$, there exist scalars $\tau_\alpha, \tau_\beta \in (0,1)$ such that $\alpha = \tau_\alpha \alpha_m + (1-\tau_\alpha)\alpha_M$ and $\beta = \tau_\beta \beta_m + (1-\tau_\beta)\beta_M$, which implies

$$\begin{aligned} \boldsymbol{\Theta}(\alpha,\beta) = {} & \tau_\alpha\tau_\beta \boldsymbol{\Theta}(\alpha_m,\beta_m) + \tau_\alpha(1-\tau_\beta)\boldsymbol{\Theta}(\alpha_m,\beta_M) \\ & + (1-\tau_\alpha)\tau_\beta \boldsymbol{\Theta}(\alpha_M,\beta_m) \\ & + (1-\tau_\alpha)(1-\tau_\beta)\boldsymbol{\Theta}(\alpha_M,\beta_M). \end{aligned}$$

Therefore, sufficient conditions for (17) are

$$\begin{aligned} &\boldsymbol{\Theta}(\alpha_m,\beta_m) \succ 0, \boldsymbol{\Theta}(\alpha_m,\beta_M) \succ 0, \\ &\boldsymbol{\Theta}(\alpha_M,\beta_m) \succ 0, \boldsymbol{\Theta}(\alpha_M,\beta_M) \succ 0. \end{aligned} \tag{18}$$

In other words, if we view $\boldsymbol{\Theta}(\alpha,\beta)$ as a point that lies within the polygon with $\boldsymbol{\Theta}(\alpha_m,\beta_m)$, $\boldsymbol{\Theta}(\alpha_m,\beta_M)$, $\boldsymbol{\Theta}(\alpha_M,\beta_m)$ and $\boldsymbol{\Theta}(\alpha_M,\beta_M)$ as vertices, then the positiveness in (17) can be assured by the positiveness of its "vertices", as in (18).

Based on the above arguments, the following relations hold true:

$$(18) \Rightarrow (17) \Rightarrow (16) \Rightarrow (15) \Rightarrow (14) \Rightarrow (11). \tag{19}$$

According to Remark 2 and (19), the control gain $\boldsymbol{K} = \boldsymbol{Y}\boldsymbol{Q}^{-1}$ can now be evaluated by solving

$$\begin{aligned} &\min_{\boldsymbol{Q},\boldsymbol{Y},\gamma} \ \gamma \\ &\text{subject to} \ \ (18) \text{ with } \rho^2 = \gamma. \end{aligned} \tag{20}$$

The optimization problem in (20) is an eigenvalue problem (EVP), which is convex with respect to variables $\boldsymbol{Q}, \boldsymbol{Y}$, and γ. We can solve (20) by using interior-point methods [12], [15].

In summary, the energy storage system in (3) is managed by using the control in (9), where the control gain $\boldsymbol{K}$ can be obtained by solving (20). In the next section, we will show the validity of the proposed energy storage management system in comparison with the case in which the stored energy state is kept constant.

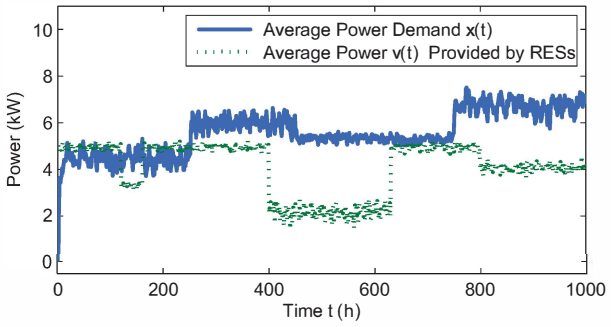

Fig. 2. Average power demand of users and the average power provided by RESs.

IV. Simulations

This section provides simulation results of our proposed storage management system. The price signal $\lambda(t)$ was simulated by

$$\lambda(t+1) = \bar{\lambda} + \eta \sum_{i=1}^{N} [\boldsymbol{u}(t)]_i \tag{21}$$

where the average price $\bar{\lambda} = 11.5$ and the scale factor $\eta = 0.16$ were chosen. The term $\sum_{i=1}^{N}[\boldsymbol{u}(t)]_i > 0$ (or $\sum_{i=1}^{N}[\boldsymbol{u}(t)]_i < 0$) represents the total power bought from (or sold to) the power grid. Referring to (21), the price signal at time t is affected by the previous power bought (or sold) at time $t-1$.

The proposed methodology (7) is compared to demand-side energy storage with a constant desired energy state achieved by using $\boldsymbol{r}(t) = (\boldsymbol{I}_N - \boldsymbol{A}_{\boldsymbol{r}})\boldsymbol{q}_m$. For convenience, we use superscripts $(\cdot)^*$ and $(\cdot)^c$ to represent all physical quantities of the proposed and the constant-state designs, respectively. That is, we have $\boldsymbol{r}(t)^* = (7)$, $\boldsymbol{q}_{\boldsymbol{r}}(t)^*$, $\boldsymbol{q}(t)^*$, $\lambda(t)^*$, and $\boldsymbol{u}(t)^*$ for the proposed design, while $\boldsymbol{r}(t)^c = (\boldsymbol{I}_N - \boldsymbol{A}_{\boldsymbol{r}})\boldsymbol{q}_m$, $\boldsymbol{q}_{\boldsymbol{r}}(t)^c$, $\boldsymbol{q}(t)^c$, $\lambda(t)^c$, and $\boldsymbol{u}(t)^c$ are for the constant-state design.

For a particular design $\boldsymbol{r}(t)$, the average power bought from or sold to the power grid is $\sum_{j=1}^{N} \frac{[\boldsymbol{u}(t)]_j}{N}$. The average money spent or earned cumulatively per user at time t can then be defined as

$$\$(\boldsymbol{u}(t)) = \sum_{t'=0}^{t} \left\{ \ \lambda(t') \times \textstyle\sum_{j=1}^{N} \frac{[\boldsymbol{u}(t')]_j}{N} \ \right\}. \tag{22}$$

The average money cumulatively saved per user by the proposed $\boldsymbol{u}(t)^*$ in contrast to $\boldsymbol{u}(t)^c$ can be evaluated as

$$\Delta\$(t) = \$(\boldsymbol{u}(t)^c) - \$(\boldsymbol{u}(t)^*) \tag{23}$$

where $\$(\boldsymbol{u}(t))$ is defined in (22).

In our simulations, the smart grid topology in Fig. 1 is considered. Fig. 2 presents the average power demand $\frac{\sum_{i=1}^{N}[\boldsymbol{x}(t)]_i}{N}$ and the average power production from RESs $\frac{\sum_{i=1}^{N}[\boldsymbol{v}(t)]_i}{N}$ versus time t. Suppose we have the physical constraints $\boldsymbol{q}(t) \in [\boldsymbol{q}_m, \boldsymbol{q}_M]$ with

$$\begin{aligned} \boldsymbol{q}_m &= \begin{bmatrix} 4.85 & 5.55 & 6.79 & 6.48 & 6.9 \end{bmatrix}^T \text{ and} \\ \boldsymbol{q}_M &= \begin{bmatrix} 8.82 & 7.66 & 11.34 & 11.28 & 10.93 \end{bmatrix}^T. \end{aligned} \tag{24}$$

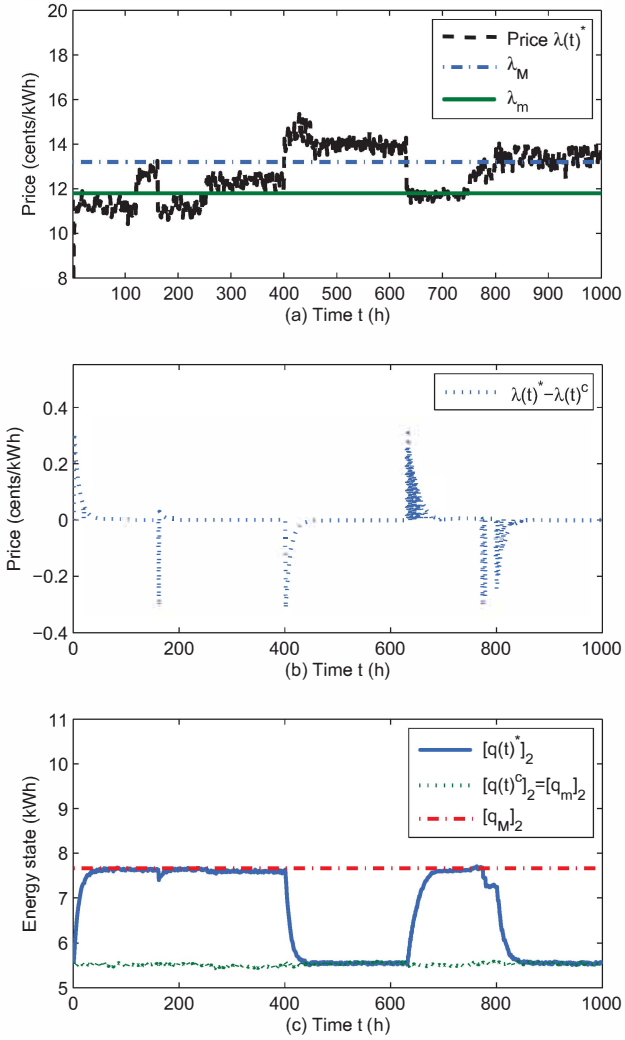

Fig. 3. Price and stored energy state: (a) price resulting from the proposed method $u(t)^*$; (b) price difference between using $u(t)^*$ and $u(t)^c$; and (c) stored energy states of different energy management systems.

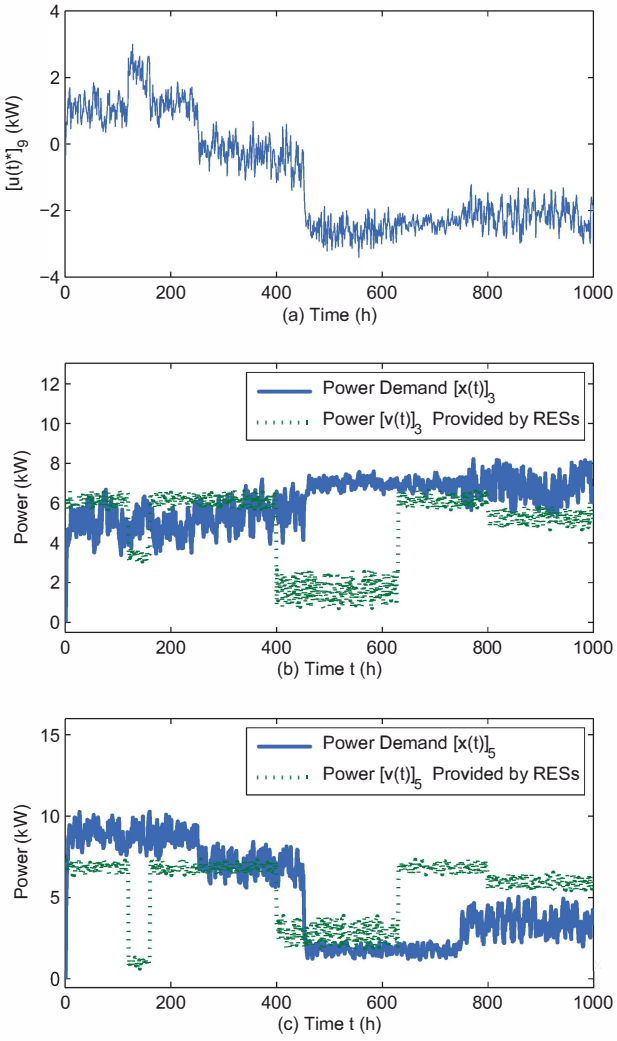

Fig. 4. Power flow on edge 9, and power demand and supply at user 3 and user 5, as shown in (a), (b) and (c), respectively. Note that positive and negative values of $[\boldsymbol{u}(t)^*]_9$ represent the same and opposite directions of power flow with respective to the directed edge, respectively.

To have a fair comparison between $\boldsymbol{u}(t)^*$ and $\boldsymbol{u}(t)^c$ using the performance index (23), we chose

$$\boldsymbol{q}(0)^* = \boldsymbol{q}(0)^c = \boldsymbol{q}_m.$$

The topology matrix $\boldsymbol{B}(0.75)$ in (2) and the storage efficiency matrix $A(0.999)$ in (3) were used with the uncertainty ranges $[\beta_m, \beta_M] = [0.7, 0.9]$ and $[\alpha_m, \alpha_M] = [0.99, 1]$, respectively.

In general, the price thresholds λ_m and λ_M in (7) depend on the price distribution $\lambda(t)$. Let $[0, t_f]$ denote the observation period. In our simulations, $t_f = 1000$ and the maximum and minimum prices

$$\lambda_u = \sup_{t\in[-t_f-1,-1]} \lambda(t) = 16 \text{ and } \lambda_\ell = \inf_{t\in[-t_f-1,-1]} \lambda(t) = 9$$

were assumed, respectively. The price thresholds

$$\lambda_m = \frac{2\lambda_u + 3\lambda_\ell}{5} = 11.8 \text{ and } \lambda_M = \frac{3\lambda_u + 2\lambda_\ell}{5} = 13.2$$

were chosen. It is noted that previous data of $\lambda(t)$ are employed to determine λ_ℓ and λ_u, which are updated periodically.

Based on (21), the price distribution obtained by using $u(t)^*$ is shown in Fig. 3(a), which is almost identical to that obtained by using $u(t)^c$, as shown in Fig. 3(b). Due to space considerations, only the energy state of user 2 is displayed in Fig. 3(c). The stored energy state in the proposed system has a negative correlation with the price signal, i.e., $\boldsymbol{q}(t)^*$ increases as the price $\lambda(t)$ decreases, and vice versa. Roughly speaking, the proposed energy management system charges batteries at low prices, while discharging batteries during a high-price period. Fig. 3 clearly shows the underlying mechanism of the proposed methodology $\boldsymbol{u}(t)^*$.

Since the proposed system involves the interaction among users, it is constructive to examine the power flow on directed edges in Fig. 1. Due to space consideration, only $[\boldsymbol{u}(t)^*]_9$ is displayed in Fig. 4(a). Positive values of $[\boldsymbol{u}(t)^*]_9$ indicate that

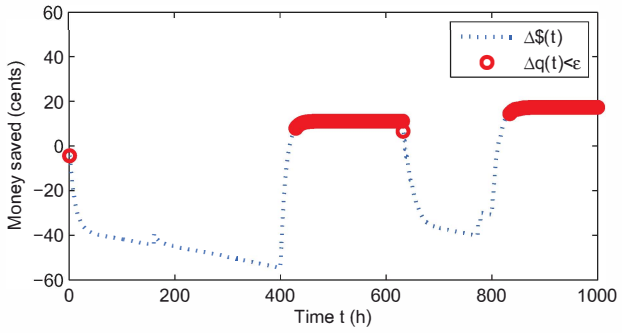

Fig. 5. Money saved, defined in (23), by using the proposed $\boldsymbol{u}(t)^*$. The period $\{t \in [0, t_f] : \boldsymbol{q}(t)^* \approx \boldsymbol{q}(t)^c = \boldsymbol{q}_m\}$ is understood as $\{t \in [0, t_f] : \Delta q(t) < \varepsilon\}$, in which $\Delta q(t) = ||\boldsymbol{q}^*(t) - \boldsymbol{q}^c(t)||$ and $\varepsilon = 0.1$. $\Delta\$(t)$ increases because the proposed storage system discharges the batteries and buys less energy than $\boldsymbol{u}(t)^c$. By contrast, the decreasing $\Delta\$(t)$ results from the situation in which batteries are charged and more energy is bought by using $\boldsymbol{u}(t)^*$ than $\boldsymbol{u}(t)^c$.

power flows from user 3 to user 5, while negative values of $[\boldsymbol{u}(t)^*]_9$ imply the reverse direction of power flow. Fig. 4(a) reflects the relation between users 3 and 5 in terms of the power demand and production, as shown in Figs. 4(b) and (c), respectively. Generally speaking, power flows from one user to another when the former has excess power while the latter lacks of it. By subtly controlling the power flow among users, power transportation between users and the power grid can be reduced and hence, yield a possible financial benefit.

Finally, the main benefit of using the proposed $\boldsymbol{u}(t)^*$ is its ability to save money, shown in Fig. 5. For a fair comparison, the periods where $\boldsymbol{q}(t)^* \approx \boldsymbol{q}(t)^c = \boldsymbol{q}_m$ are primarily considered. Fig. 5 shows that, during these periods, $\Delta\$(t)$ is always positive and its value continually increases upon increasing t. Therefore, the longer the observation time is, the more money can be saved by the proposed methodology. In conclusion, the proposed energy storage system results in a more economical way for energy management as compared to the constant-state energy storage system $\boldsymbol{u}(t)^c$.

V. Conclusion

An economical energy storage system for the smart grid has been proposed. This system involves energy production capabilities of users and considers energy losses owing to storage and transportation as well as uncertainties concerning these values. The proposed system has been designed by using an H_∞ design, which brings a useful tool from the control community to the smart grid community.

Our simulations have shown that the proposed system can generate a financial benefit in the long term as compared to a storage system that always keeps the same energy level. The underlying idea is to charge batteries at a low price, while discharging them at a high price. Interesting future research may include a tailored design on the price thresholds according to different price distributions, and further analysis of the costs of storage and transportation.

References

[1] K. Pollhammer, F. Kupzog, T. Gamauf, and M. Kremen, "Modeling of demand side shifting potentials for smart power grids," in *Proc. IEEE Africon*, Livingstone, Zambia, Sep. 2011, pp. 1–5.

[2] Z. Zhu, J. Tang, S. Lambotharan, W. H. Chin, and Z. Fan, "An integer linear programming based optimization for home demand-side management in smart grid," in *Proc. IEEE PES Innovative Smart Grid Technologies Conference*, Washington, DC, USA, Jan. 2012, pp. 1–5.

[3] H. K. Nguyen, J. B. Song, and Z. Han, "Demand side management to reduce peak-to-average ratio using game theory in smart grid," in *Proc. IEEE Int. Conference on Computer Communications Workshops*, Orlando, FL, USA, Mar. 2012, pp. 91–96.

[4] A. Mohsenian-Rad, V. Wong, J. Jatskevich, R. Schober, and A. Leon-Garcia, "Autonomous demand-side management based on game-theoretic energy consumption scheduling for the future smart grid," *IEEE Trans. Smart Grid*, vol. 1, no. 3, pp. 320–331, Dec. 2010.

[5] S. Bashash and H. K. Fathy, "Modeling and control insights into demand-side energy management through setpoint control of thermostatic loads," in *Proc. American Control Conference*, San Francisco, CA, USA, June-July 2011, pp. 4546–4553.

[6] A. Fazeli, E. Christopher, C. M. Johnson, M. Gillott, and M. Sumner, "Investigating the effects of dynamic demand side management within intelligent smart energy communities of future decentralized power system," in *Proc. IEEE PES Int. Conference and Exhibition on Innovative Smart Grid Technologies*, Manchester, UK, Dec. 2011, pp. 1–8.

[7] H. Dagdougui, R. Minciardi, A. Ouammi, and R. Sacile, "Optimal control of a regional power microgrid network driven by wind and solar energy," in *Proc. IEEE Int. Systems Conference*, Montreal, Quebec, Canada, Apr. 2011, pp. 86–90.

[8] W.-Y. Chiu, H. Sun, and H. V. Poor, "Robust power flow control in smart grids with fluctuating effects," in *Proc. IEEE Int. Conference on Computer Communications Workshops*, Orlando, FL, USA, Mar. 2012, pp. 97–102.

[9] Z. M. Fadlullah, Y. Nozaki, A. Takeuchi, and N. Kato, "A survey of game theoretic approaches in smart grid," in *Proc. Int. Conference on Wireless Communications and Signal Processing*, Nanjing, China, Nov. 2011, pp. 1–4.

[10] G. Mine, T. Handa, T. Tachikawa, Y. Watanabe, J.-I. Ichimura, and H. Nishi, "Evaluation of cooperative demand control system on micro grid," in *Proc. Annual Conference of the IEEE Industrial Electronics Society*, Porto, Portugal, Nov. 2009, pp. 3593–3598.

[11] W. Saad, Z. Han, and H. V. Poor, "Coalitional game theory for cooperative micro-grid distribution networks," in *Proc. IEEE Int. Conference on Communications Workshops*, Kyoto, Japan, Jun. 2011, pp. 1–5.

[12] S. Boyd, L. El Ghaoui, E. Feron, and V. Balakrishnan, *Linear Matrix Inequalities in System and Control Theory*. Philadelphia, PA: SIAM, 1994.

[13] W.-Y. Chiu and B.-S. Chen, "Multisource prediction under nonlinear dynamics in WSNs using a robust fuzzy approach," *IEEE Trans. Circuits Syst. I*, vol. 58, no. 1, pp. 137–149, Jan. 2011.

[14] H. D. Tuan, P. Apkarian, T. Narikiyo, and Y. Yamamoto, "Parameterized linear matrix inequality techniques in fuzzy control system design," *IEEE Trans. Fuzzy Syst.*, vol. 9, no. 2, pp. 324–332, Apr. 2001.

[15] S. Boyd and L. Vandenberghe, *Convex Optimization*. New York: Cambridge Univ. Press, 2004.